Friction between Cellulose Surfaces and Effect of Xyloglucan Adsorption

Johanna Stiernstedt,[†] Harry Brumer, III,[‡] Qi Zhou,[‡] Tuula T. Teeri,[‡] and Mark W. Rutland*[,†]

Department of Chemistry, Surface Chemistry, Royal Institute of Technology, SE-100 44 Stockholm, Sweden and Institute for Surface Chemistry, Box 5607, SE-114 86 Stockholm, Sweden, and Department of Biotechnology, Royal Institute of Technology, AlbaNova University Center, SE-106 91 Stockholm, Sweden

Received February 3, 2006; Revised Manuscript Received April 10, 2006

The forces and friction between cellulose spheres have been measured in the absence and presence of xyloglucan using an atomic force microscope. The forces between cellulose are monotonically repulsive with negligible adhesion after contact is achieved. The friction coefficient is observed to be unusually high in comparison with other nanotribological systems. We have confirmed that xyloglucan adsorbs strongly to cellulose, which results in a much stronger adhesion, which is dependent on the time the surfaces are in contact. Xyloglucan also increases the repulsion on approach of the cellulose surfaces, and the friction is markedly reduced. The apparently incompatible observations of decreased friction in combination with increased adhesion fulfills many of the necessary criteria for a papermaking additive.

Introduction

Xyloglucan is a polysaccharide found in the plant cell wall that is generally believed to cross-link load-bearing cellulose microfibrils and affect wall mechanical properties.[1−4] Indeed, many studies have shown that xyloglucan adsorbs strongly to cellulose,[5−9] and recently, this specific interaction has been harnessed in the development of a new versatile method to functionalize cellulosic surfaces.[10,11]

One major application for cellulose fibers is papermaking. Naturally occurring xyloglucan is extracted during the pulping process; however, attempts have been made to add xyloglucan to the pulp before the paper sheet is formed, with an approximately 20−30% increase in the tensile strength of paper as a result.[12,13] Another benefit of xyloglucan addition to pulp is that the paper becomes smoother as a result of better paper formation.[12] It has been speculated that the increased paper strength is a result of stronger cellulose−cellulose joints and that the paper formation is improved by reduced friction between the fibers.[12]

Such measurements and inferences are of course based on macroscopic studies of the paper as a whole. To explain the impact of xyloglucan on better formation on one hand and on increased paper strength on the other hand, it would be useful to study the effect of xyloglucan at a single contact and attempt to explain the mechanisms of these two effects. For example, reduced friction is usually associated with reduced adhesion, so it is not a priori obvious whether the reported formation benefit is indeed associated with reduced friction, and if so whether this is because of, or despite, the apparently enhanced adhesion.

Measurement of, for example, the adhesion between individual fibers is possible using an atomic force microscope (AFM) in crossed fiber configuration (one of the fibers is glued to the cantilever and one to the underlying substrate), but the complexity of the fiber surface and its swelling behavior renders both the interpretation and the reproducibilty of such measurements challenging. An alternative route is to measure the interactions between model cellulose surfaces using the surface force apparatus (SFA)[14−16] or the AFM[17−23] and study the effect of additives on the model joint. In these works, the following general observations have been made. Long-range forces between cellulose surfaces generally follow the Poisson−Boltzmann (PB) theory for electrostatic repulsion. Most studies also report an additional short-range repulsion, which however, has different ranges in different studies. Also, the explanation of the origin of the short-range repulsion varies between studies, and it has been attributed to dangling tails, to compression and dehydration of a highly solvated surface region, and to surface roughness. The only exception is one measurement by Notley et al.,[21] which was made at low pH where cellulose is uncharged and hence shows van der Waals attractions.

It has been shown by a number of authors that the precontact forces, due to, for example, steric layers, profoundly influence the frictional forces observed.[24−26] To summarize broadly, the requirement for friction benefit in steric systems is a steeply repulsive, but nonetheless short-ranged, steric force with a well-defined slipping plane.

To adequately examine the effects of xyloglucan on cellulose, an examination of the precontact forces on approach (relevant to formation), the forces on separation (adhesion), and the lateral force−load relationship (friction) are here undertaken in two types of cellulosic contacts.

Experimental Procedures

The atomic force microscope employed in this work is a Nanoscope III AFM (Veeco), extended with a closed loop PicoForce unit. The PicoForce unit measures the position of the driving piezocrystal, giving independent information of the movement of the surface, which makes the PicoForce AFM very suitable for force measurements. Force measurements were performed using the colloidal probe technique of

* To whom correspondence should be addressed. E-mail: mark.rutland@surfchem.kth.se; phone: +46 8 790 99 14; fax: +46 8 20 89 98.

[†] Royal Institute of Technology and Institute for Surface Chemistry.

[‡] AlbaNova University Center.

10.1021/bm060100i CCC: $33.50
Published on Web 05/27/2006

Ducker et al.[27,28] The cantilevers used were uncoated, tipless, rectangular silicon cantilevers (MicroMasch, Tallinn, Estonia), with regenerated cellulose beads (Kanebo, Japan, made by the viscose process), attached in-house with Casco Araldite Rapid epoxy adhesive. Details of the bead properties, source, and attachment procedure are given in an earlier publication[18]—as a result of their preparation, they are likely to differ somewhat in terms of properties such as crystallinity, molar mass, and surface chemistry to pulp fiber surfaces. The normal force constant of the cantilevers was calibrated using the method of Cleveland et al.,[29] and the dimensions of the cellulose beads were measured in a light microscope (Nikkon). All measurements were performed in Milli-Q water with 0.1 mM NaCl at pH 5.8. Xyloglucan from tamarind (*Tamarindus indica*) seed (Megazyme, Bray, Ireland) had a monosaccharide composition of Xyl/Glc/Gal/Ara = 35:45:16:4, according to the supplier's specification. Xyloglucan was dissolved in Milli-Q water (1 mg/mL) and was allowed to adsorb to cellulose materials overnight.

Friction was measured as a function of increasing and decreasing loads with a scan size of 2 μm and a scan rate of 0.5 Hz. Prior to the experiments, the lateral force constants of the cantilevers were calibrated.[30,31] Both frictional and normal force measurements followed the recommended approach from an IUPAC technical report.[32]

Forces and friction were measured either between two cellulose beads or between a bead and a solvent cast cellulose film. In the former case, one bead was employed as a colloidal probe, and the other was glued to a mica surface. The radius of curvature of the interaction, R, was calculated by

$$R = \frac{R_1 R_2}{R_1 + R_2} \quad (1)$$

where R_1 and R_2 are the radii of the two cellulose beads. For the case of measurements between a cellulose colloidal probe and a solvent cast cellulose film, the radius of interaction equals the radius of the colloidal probe.

The zero of separation is not absolute in AFM measurements but is defined as the point where the spring deflection follows the piezo extension, often referred to as the region of constant compliance or hard wall contact. To estimate a value of the surface potential, the forces were fitted with DLVO theory.[33,34] The van der Waals attraction was estimated with a Hamaker constant[35] of 8×10^{-21} J, and the nonlinear Poisson−Boltzmann equation was solved numerically, using the algorithm by Chan et al.,[36] which provides the electrical double layer repulsion.

Results

Forces on Approach. Figure 1 shows the normalized force−distance profiles between two cellulose spheres in solutions of 0.1 mM NaCl, 1 mg/mL xyloglucan (XG), and 0.1 mM NaCl after rinsing away any nonadsorbed XG, on a logarithmic scale. In all solutions, the interaction between the spheres is purely repulsive on approach, and no attractive van der Waals force is observed at small separations. The effect of XG on the interaction profile is clearly evident; there is a significant increase in the range and magnitude of the repulsive force upon addition of XG, and it does not change appreciably after rinsing. The lower curve approaches the resolution of the AFM, and so, in this case only, the depicted curve is the average of 10 measurements.

For all solutions, two distinct repulsive force regimes are observed, a short-range electrosteric force and a long-range electrostatic force. The long-range force was found to be consistent with the Poisson−Boltzmann theory. No van der Waals attraction is seen on approach of the surfaces but is nevertheless observed on separation. Hence, the data in Figure 1 are fitted with DLVO theory using a Hamaker constant[35] of

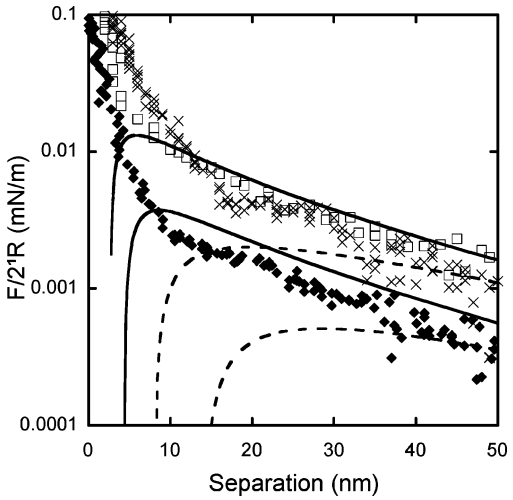

Figure 1. Force curves on approach between two cellulose spheres in solutions of 0.1 mM NaCl (filled diamonds), 1 mg/mL XG (open squares), and after rinsing with 0.1 mM NaCl (crosses) plotted on a logarithmic scale. The lines are fits of DLVO theory to the data, with a surface potential of −8 mV for the lower set of lines and −13 mV for the upper set of lines. The solid lines represent the constant charge boundary condition, and the dashed lines represent the constant potential boundary condition. The Debye length was 30 nm for both fits (calculated value, not a fitting parameter).

8×10^{-21} J. The solid lines show the constant charge boundary condition of DLVO theory, and the dashed lines show the constant potential boundary condition. The lower set of lines represents a surface potential of −8 mV and the upper set of lines a potential of −13 mV. Both fits have a Debye length of 30 nm, which is the calculated value for 0.1 mM salt, and hence not a fitting parameter. The sign of the potential cannot be directly obtained from the DLVO fitting, but zeta-potential measurements of cellulose show that cellulose is negatively charged above pH 3.[37] The surface potential increases with addition of XG. After rinsing, the surface potential remains unchanged, indicating that the XG is irreversibly adsorbed.

In the fits, the plane of charge is assumed to occur at the hard wall, although a plane of charge is not well-defined for cellulose systems. Therefore, due to ambiguity, both in the position of zero separation and location of plane of charge, the DLVO fits should only be regarded as guidelines, although what is completely clear is that the surface potential and corresponding surface charge are very low. Previously reported values of fitted potentials at comparable pH and salt concentrations are −9,[22] −11,[38] −17,[18] and −21 mV;[19] however, the same uncertainty is valid for these previously reported values as in the present study. If the plane of charge were in fact to be located at the onset of the steric repulsion, then the surface potential obtained from fitting would be even lower. Even if the effective charge distributions were very different for the two cases, the surface charge for the XG case is significantly larger.

The surface charge of cellulose probably originates from the dissociation of carboxylic groups introduced during the pulping process,[39] and cellulose model surfaces have different surface charges depending on the properties of the pulp they are made from and other treatments such as the viscose process. XG, on the other hand, contains no carboxylic acids and is thus expected to be uncharged. (Charging XG from rose has been observed but in that case is probably the result of tight binding to acidic pectin,[40] which cannot be the case here.) The highly substituted parts of XG are thought not to bind to cellulose but instead form loops and make XG more bulky. The presence of unbound groups probably renders the polymer more mobile and increases

the probability of chain end detachment and reattachment to an opposing surface, thereby facilitating cross-linking between cellulose fibers.[7] Such loops increase the repulsion on approach. The binding of XG to cellulose renders the surface molecules more compatible with water, which in turn allows the apparent surface charge to increase slightly, and consequently, the double layer component of the force becomes somewhat larger.[18]

DLVO theory predicts that the surfaces should jump into contact at small separations; however, instead, a short-range electrosteric repulsion was observed in all cases. The range of the electrosteric repulsion becomes longer when the XG solution is added, and it decreases only slightly in range after rinsing, suggesting that only a small fraction of the XG is so loosely adsorbed that it desorbs on dilution. XG chains, being water-soluble, extend further out in the solution than the insoluble cellulose chains, thereby increasing the electrosteric repulsion.

This short-range electrosteric repulsion has been observed previously for cellulose.[14,18,19,23] However, the range of the repulsion varies in the literature, and there is as yet no clear picture of its origin. The extent of the steric repulsion increases with increasing pH (increased charging and swelling of cellulose)[18,21] and decreases with increasing salt concentration (decreased repulsion between cellulose chains);[18] therefore, the solvent conditions may be one reason for the differences in the reported values of the range of the steric repulsions.

It is difficult to say if the repulsion is a result of compression and dehydration of a highly solvated surface region[18] or if a dangling tails model[14] is more appropriate. In both these cases, the repulsion can be thought of as having a steric nature. The short-range repulsion collapses at high ionic strength,[18] implying that any surface steric layer is associated with charging of the cellulose chains, and at low pH when the cellulose is uncharged, the jump into van der Waals attraction is very clear.[21] Zauscher and Klingenberg[19] argue that the steric repulsion may actually be an artifact of the surface roughness of the substrates; however, no dependence on surface roughness has been observed for the repulsion between cellulose surfaces,[41] and this argument does not explain the collapse of the repulsion at high salt concentrations. There is essentially very little more that can be done to throw more light on this interaction, and based on the previous discussion, we will here refer to the interaction as an electrosteric force.

The curves in Figure 1 were taken at 0.2 μm/s, and the curve for the bare cellulose surfaces is redrawn in Figure 2. At this rate, the hydrodynamic repulsion is negligible (dotted line in Figure 2); however, at 2 μm/s, the long-range repulsion increases as seen in Figure 2, where the hydrodynamic repulsion is plotted as the solid line. The inset shows that the difference in the repulsion due to rate is accounted for by the hydrodynamic equation[42]

$$F_{\mathrm{H}} = -\frac{6\pi\eta R^2 \mathrm{d}D}{D \quad \mathrm{d}t} \qquad (2)$$

where η is the viscosity, D is the separation between the two slip planes, dD/dt is the relative rate of approach of the two surfaces, and R is the radius of curvature (defined in eq 1). This equation is valid as long as the two radii used in the calculation of R are approximately the same.

The application of eq 2 to the data is entirely sufficient to correct for the effect of hydrodynamics, using the bulk value for the viscosity of water. This has several implications. First, the zero of separation obtained from constant compliance must be a reasonable approximation of the sticking plane (where the velocity of the water goes to zero, so-called wall stick). Second, there can be no significant shift in the position of the sticking plane as the separation of the surfaces changes (i.e., due to compression of the electrosteric layer). Finally, forced percolation through a gel-like layer is not a significant contributing effect. (For thick, swollen polyelectrolyte films, a significant increase in the effective viscosity can be observed.[25])

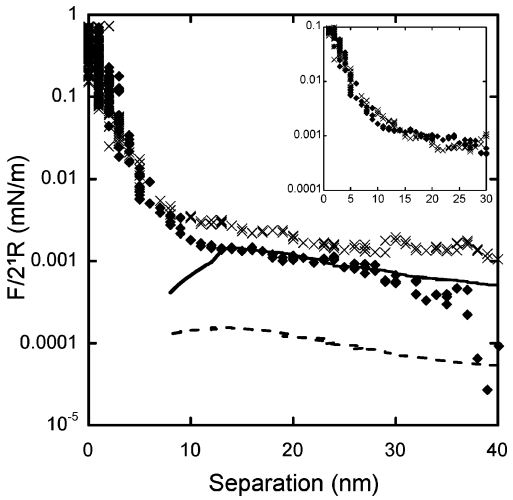

Figure 2. Force curves on approach between two cellulose spheres at different driving rates in a solution of 0.1 mM NaCl. The rates are 0.2 μm/s (filled diamonds) and 2 μm/s (crosses). The solid line represents the calculated hydrodynamic force at 2 μm/s and the dotted line at 0.2 μm/s. The inset shows the interaction profiles with the calculated hydrodynamic force removed.

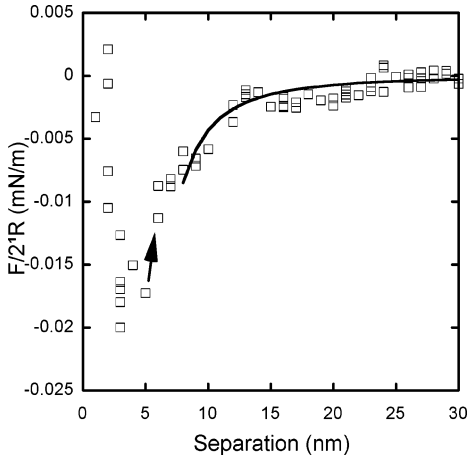

Figure 3. Force curve on separation between two cellulose spheres in a solution of 0.1 mM NaCl. The solid line is a fit of van der Waals theory with a Hamaker constant of 8×10^{-21} J. The arrow, which has a slope identical to the spring constant, indicates the jump out of contact.

Forces on Separation. Figure 3 shows the forces measured on separation of two cellulose spheres in a solution of 0.1 mM NaCl. A small adhesion is observed on separation; the surfaces jump apart from a position of 5 nm out from hard wall contact. The arrow, indicating the jump out of contact, has a slope of 50 kN/m^2, which corresponds well to the cantilever spring constant (0.2 N/m) divided with the radius of interaction (3.69 μm) being 54.2 kN/m^2. The jump out is due to a spring instability that occurs when the energy stored in the spring is greater than the adhesive force. Thus, the points recorded by the instrument, with a 2.5 ms interval, have a gradient corresponding to the spring constant. The surfaces jump apart into an attractive force profile, which follows van der Waals predictions (solid line) with a Hamaker constant of 8×10^{-21} J[35]

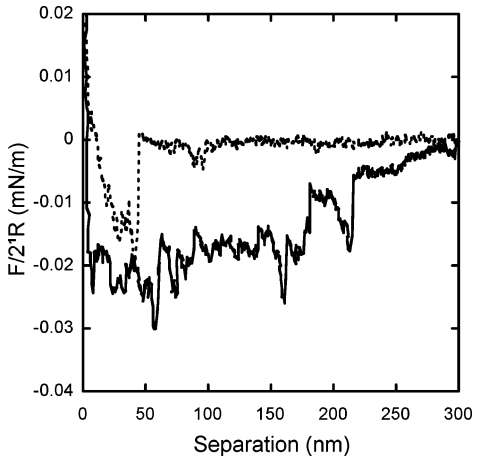

Figure 4. Force curves on retraction between two cellulose spheres in a solution of 1 mg/mL XG for two different times in contact. The dotted time represents 1 s in contact, and the solid line 100 s.

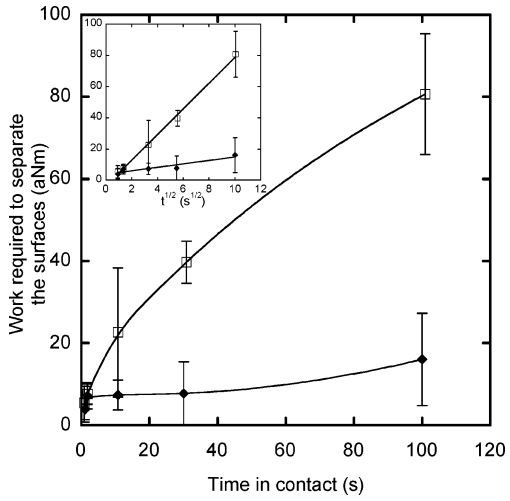

Figure 5. Work required to separate the surfaces as a function of contact time for two cellulose spheres in solutions of 0.1 mM NaCl (closed diamonds) and 1 mg/mL XG (open squares). The inset shows the adhesion as a function of $t^{1/2}$. The lines are added to guide the eye.

and the plane of interaction placed at the point of maximum adhesive force (which is 3 nm from nominal hard wall contact).

No jump into adhesive contact is seen on approach of the surfaces; instead, there is compression and dehydration of the water swollen surface layer. During the time scale of the separation, the cellulose is not able to rehydrate, which is why the measurement is slightly hysteretic. Notley et al.[21] observed a van der Waals attraction on approach as well as a separation for similar measurements but at a lower pH. Under such conditions, cellulose is uncharged, which removes the electrostatic repulsion and significantly reduces the swelling that in our case masks the van der Waals attraction on approach.

The forces on separation in 1 mg/mL XG are presented in Figure 4. The dashed curve represents the interaction in XG at a rate of 0.2 μm/s, and the solid curve represents the interaction under the same conditions but with 100 s prolonged time in contact. The adhesion is larger in the presence of XG as compared to the bare cellulose surfaces, and the adhesion is very sensitive to the time in contact, which is further shown in Figure 5. In the presence of XG, the surfaces jump apart to a position well beyond the range of the surface force. The adhesion is a result of the specific binding between cellulose and XG as indicated by the saw-tooth pattern, which is typical for the pull-off of individual chains, commonly seen between surfaces with adsorbed polymers.[43,44] The interaction profile is very irregular, indicating that a large number of cellulose−XG bonds with different contour lengths are present.

Bridging adhesion between two surfaces in a polymer solution occurs when the polymer has large attraction to both surfaces, and it has been measured as early as 1979.[45] The AFM has been used for measuring such discrete adhesive interactions since 1992,[46] after which pioneering work was done in biological systems.[47,48] Extensive work of proteins, polysaccharides, and DNA has shown long-range adhesion and pull-off of individual chains (e.g., see the following two reviews).[43,44] Later, some adhesion studies have been performed on cellulose substrates with wet strength additives,[49] cellulose binding modules,[50] and XG.[51] In all of these studies, there was a small adhesion between bare cellulose surfaces in water, which increased in the presence of the additives. For the wet strength additives (which were of polymeric origin) and XG, the pull-off of individual chains was clearly evident. Unfortunately, none of these studies shows any inward curves on a logarithmic scale; therefore, no conclusions can be drawn regarding the forces on approach.

Figure 5 shows the work required to separate the surfaces as a function of time in contact, in the presence and absence of XG. The adhesion in the presence of XG increases dramatically with increased time in contact. The inset shows the work required to separate the surfaces plotted as a function of $t^{1/2}$ with which it is clearly linear, suggesting that the adhesion is controlled by a diffusion process.[52,53] This is consistent with parts of XG chains diffusing to the opposing cellulose surface and creating cross-links. The time-dependent adhesion, together with its clear sawtooth pattern in Figure 4, provides strong evidence for bridging of XG between cellulose surfaces. The adhesion appears to also increase with time in contact for the bare cellulose surfaces, but the effect is far smaller than in the presence of XG, and the error bars are such that this effect is inconclusive.

Recent studies have shown that the tensile strength of paper increases about 30% with the addition of XG,[12,13] and Christiernin et al.[12] attribute the increased paper strength to increased adhesion of each fiber−fiber joint; they have not seen any evidence for an increased number of joints. The observation of bridging adhesion documented here is entirely consistent with that interpretation.

Friction. In Figure 6, the lateral friction as a function of applied load is shown for a cellulose sphere sliding against another sphere, immersed in 0.1 mM NaCl in the presence and absence of 1 mg/mL XG. The friction is zero for zero applied load for all measurements, and the friction follows Amontons' law

$$F_f = \mu L \tag{3}$$

where F_f is the friction force, L is applied load, and μ is the friction coefficient. Amontons' law is generally valid for multiasperity contact and nonadhesive systems, in which case the contact area is proportional to the applied load. (For adhesive systems, the adhesion effectively adds to the applied load, and a modified form of Amontons' law should be used.[54−58])

The friction coefficient is highest for the bare cellulose, $\mu = 1.02$, and it decreases by almost a factor of 2 in the presence of XG, $\mu = 0.61$. The friction coefficient does not change significantly after rinsing, providing further evidence that the XG molecules are not rinsed away and that it is the bound XG and not the loosely bound that reduces the friction.

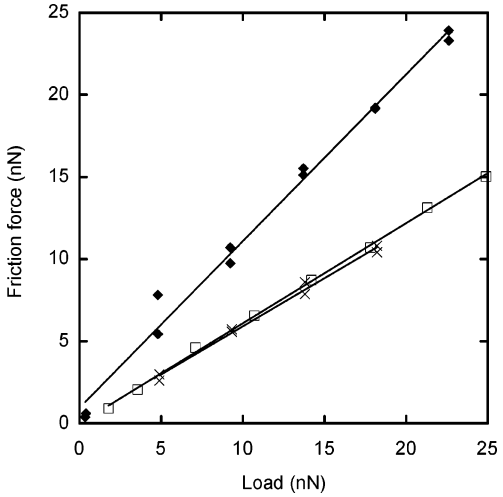

Figure 6. Friction force as a function of applied load for two cellulose spheres in solutions of 0.1 mM NaCl (closed diamonds), 1 mg/mL XG (open squares), and 0.1 mM NaCl after rinsing (crosses). The solid lines represent the friction coefficients, which are $\mu = 1.02$ in NaCl, $\mu = 0.61$ in XG, and $\mu = 0.59$ after rinsing.

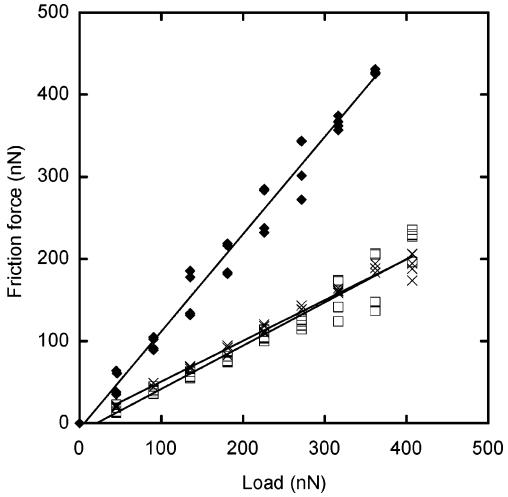

Figure 7. Friction as a function of applied load for a cellulose sphere and a solvent cast cellulose film in solutions of 0.1 mM NaCl (closed diamonds), 1 mg/mL XG (open squares), and 0.1 mM NaCl after rinsing (crosses). The solid lines represent the friction coefficients, being $\mu = 1.18$ in NaCl, $\mu = 0.53$ in XG, and $\mu = 0.50$ after rinsing.

Our values of friction coefficients for bare cellulose agree well with values of Theander et al.[23] who report friction coefficients just above 1 for two cellulose spheres. Zauscher and Klingenberg,[20] have measured friction coefficients about 0.6 for a cellulose sphere sliding over a flat cellulose surface. We note that the friction coefficient depends critically on the torsional spring constant used for the measurement and that manufacturer's specifications can often be as much as a factor of 2 out. Friction coefficients are very dependent on surface roughness,[59] and since the surfaces used in that study have a lower roughness, it is not unreasonable that they should display lower friction. A comparison between different cellulose model surfaces, with respect to friction, surface roughness, and surface forces, is the subject of a forthcoming publication.[41]

The friction decreases by almost 50% with the addition of XG, a reduction that we have found to be very reproducible. The question remains, however, as to the mechanism of the friction reduction. Increased adhesion is generally associated with increased friction,[54−58] and the system becomes more adhesive in the presence of XG. Now, the adhesion is present first after the surfaces have been brought into close contact and water has been expelled from the contact zone, and in the presence of XG, the adhesion increases significantly with increasing time in contact. Presumably, as the surfaces are sliding past each other, the XG molecules do not have time to bind to the opposing surface since the sliding rate is fast as compared to the time scales required for bridging. If bridging were able to occur during the time scale of the measurements, then it would indeed increase the friction force.[25]

On approach, however, there is repulsion, which increases in the presence of XG, and an increased repulsion between the surfaces is generally associated with a decrease of the measured friction.[24] The XG molecules effectively create a boundary lubricating layer, which imparts a steep repulsive force. It is also possible that the XG molecules create a well-defined slipping plane between the cellulose surfaces.

Solvent Cast Cellulose Film. Friction has also been measured between a cellulose sphere and a solvent cast cellulose film, and these results are presented in Figure 7. The friction coefficients are $\mu = 1.18$ for the bare cellulose surfaces, $\mu = 0.53$ in the presence of XG, and $\mu = 0.50$ after rinsing, which agrees well with the case of two cellulose spheres. The friction reduction caused by XG is even greater in this case. The fact that the friction results agree so well implies that at a given load, the nature of the contact and friction mechanisms are similar for the two cases. The solvent cast film is rather different in character to the spheres in its swelling behavior, and this fact is reflected in the normal forces.

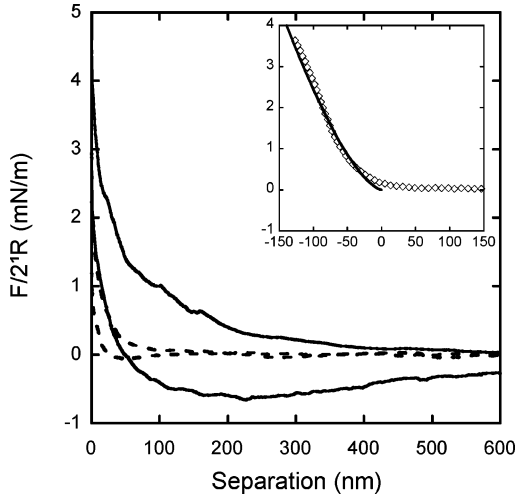

Figure 8. Force−distance profiles between a cellulose sphere and a solvent cast cellulose film in solutions of 0.1 mM NaCl (dashed lines) and 1 mg/mL XG (solid lines). The inset shows the recalculated (see text) force curve on approach in 0.1 mM NaCl (diamonds) and a Hertzian fit with $K = 1.7$ MPa (solid line). For clarity, only every 20th data point is plotted.

Figure 8 shows the force data for the solvent cast film in the presence (solid lines) and absence (dashed lines) of XG. The range and magnitude of the repulsive force increase with the addition of XG, which is in agreement with the sphere−sphere case. However, the increase is much larger, and this is due to continual swelling of the cast film with time, which is unavoidable. We note that the solvent cast cellulose film is very soft and highly swollen in water, and this is reflected by significant deformation under an applied load. This deformation is manifested by apparently long-range forces. In an attempt to estimate the deformation, the force curve in the bare cellulose case was reanalyzed using the gradient of constant compliance from the calibration measurement when neither the cellulose

particle nor the cellulose film was present. The zero of separation was determined from the point where the slope of the force curve begins to increase rapidly since the constant compliance regime is unreliable for determining contact in compressive systems.[60] The reanalyzed curve, plotted in the inset of Figure 8, was then fitted with the Hertz theory,[61] which predicts the contact area, a, and central displacement, δ, for two nonadhering surfaces in contact.

$$a^3 = RF/K \tag{4}$$

$$\delta = a^2/R = F/Ka \tag{5}$$

$$\frac{1}{K} = \frac{3}{4}\left[\frac{1-\nu_1^2}{E_1} + \frac{1-\nu_2^2}{E_2}\right] \tag{6}$$

where R is the radius of curvature of interaction, F is the applied force, K is the reduced elastic modulus, υ_n is the Poisson ratio for each surface, and E_n is the elastic modulus for each surface. The fitted K value of 1.7 MPa is significantly lower than the elastic modulus of 22 MPa for a cellulose sphere in humid air but is in agreement with estimations of a gel-like surface layer of a cellulose fiber, where $E \approx 1-5$ MPa.[62] As seen in the inset of Figure 8, the majority of the repulsion is explained by elastic deformation; however, there is still a repulsive force not accounted for by the Hertzian fit. This is of course the surface forces including double layer and any steric contributions. There may also be some contribution from assuming a single elastic modulus for the film. It is likely that in fact the elastic modulus varies with depth into the film,[60] and this is certainly the case for longer swelling times where a fit such as in Figure 8 cannot be achieved due to a steeply varying elastic constant. The degree of swelling is closely related to the crystallinity of the cellulose, and the extremely long-range apparent force in the case of the solvent cast cellulose film suggests that the film is amorphous.

Deformation of the substrates will, if not taken into account as in the analysis as stated previously, be manifested as an extra repulsion;[60] however, there is only a small effect on the true precontact forces, which are marginally overestimated.

A consequence of the soft surface is that much larger adhesion forces are measured. This may be related to the increased possibility of bridging, due to the 3-D nature of the cast film or a larger area of contact. The work required to separate the surfaces versus contact time is presented in Figure 9. The inset once again shows the work required to separate the surfaces as a function of $t^{1/2}$, and the linear relationship is reminiscent of that in Figure 5, which confirms that the bridging of XG to cellulose is diffusion controlled.

This resemblance in time dependence of the adhesion together with the fact that the friction behavior agrees between the two sets of cellulose surfaces indicates that the final cellulose−cellulose contacts are comparable.

Conclusion

Surface force measurements clearly confirm that xyloglucan adsorbs irreversibly to cellulose. An important effect of the xyloglucan adsorption is that the very small adhesion between cellulose surfaces in water is significantly increased due to the bridging and formation of specific bonds of xyloglucan to both surfaces. This provides a possible mechanistic explanation for the recent observation that the tensile strength of paper increases by about 30% by the addition of xyloglucan.[12,13]

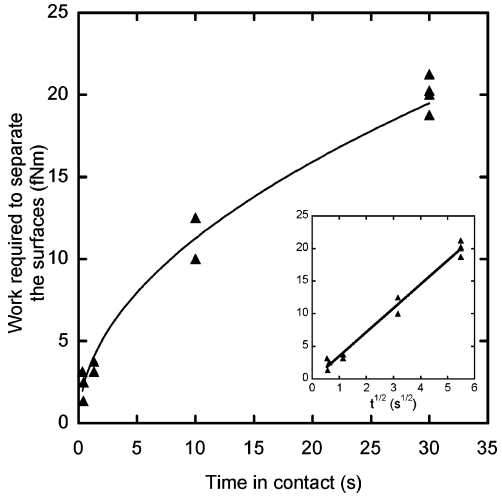

Figure 9. Work required to separate the surfaces as a function of contact time for a cellulose sphere and a solvent cast cellulose film in a solution of 1 mg/mL XG. The inset shows the work of adhesion as a function of $t^{1/2}$. The lines are added to guide the eye.

The present results also show that the adsorbed xyloglucan significantly reduces friction, giving support to the view that the improved formation is indeed due to beneficial friction properties imparted by xyloglucan. It would appear that xyloglucan is thus in many ways an ideal additive since it combines apparently incompatible characteristics. The friction reduction is associated with the increased repulsion between the cellulose surfaces, whereas the strength is imparted by increased adhesion (attractive). The apparent conundrum is resolved by the fact that the bridging forces have a much longer relaxation time than sliding residence times and that the adhesion is only activated after the surfaces are forced into contact, which in the case of paper occurs as capillary forces drive the fibers into intimate contact during drying.

Acknowledgment. This work was financed by the KTH Biofiber Materials Centre (BiMaC) and the Swedish Research Council (Vetenskapsrådet), whom we gratefully acknowledge. H.B. and M.W.R. are Fellows of the Swedish Research Council (Rådsforskare).

References and Notes

(1) Cosgrove, D. J. *Nat. Rev. Mol. Cell Biol.* **2005**, *6*, 850−861.
(2) Hayashi, T. *Annu. Rev. Plant Physiol. Plant Mol. Biol.* **1989**, *40*, 139−168.
(3) Chanliaud, E.; De Silva, J.; Strongitharm, B.; Jeronimidis, G.; Gidley, M. J. *Plant J.* **2004**, *38*, 27−37.
(4) Fry, S. C. *J. Exp. Bot.* **1989**, *40*, 1−11.
(5) Hayashi, T.; Maclachlan, G. *Plant Physiol.* **1984**, *75*, 596−604.
(6) Levy, S.; York, W. S.; Stuikeprill, R.; Meyer, B.; Staehelin, L. A. *Plant J.* **1991**, *1*, 195−215.
(7) Hayashi, T.; Ogawa, K.; Mitsuishi, Y. *Plant Cell Physiol.* **1994**, *35*, 1199−1205.
(8) Whitney, S. E. C.; Brigham, J. E.; Darke, A. H.; Reid, J. S. G.; Gidley, M. J. *Plant J.* **1995**, *8*, 491−504.
(9) Vincken, J. P.; Dekeizer, A.; Beldman, G.; Voragen, A. G. J. *Plant Physiol.* **1995**, *108*, 1579−1585.
(10) Brumer, H., III; Zhou, Q.; Baumann, M. J.; Carlsson, K.; Teeri, T. T. *J. Am. Chem. Soc.* **2004**, *126*, 5715−5721.
(11) Zhou, Q.; Greffe, L.; Baumann, M. J.; Malmstrom, E.; Teeri, T. T.; Brumer, H., III *Macromolecules* **2005**, *38*, 3547−3549.
(12) Christiernin, M.; Henriksson, G.; Lindstrom, M. E.; Brumer, H., III; Teeri, T. T.; Lindstrom, T.; Laine, J. *Nordic Pulp Paper Res. J.* **2003**, *18*, 182−187.
(13) Lima, D. U.; Oliveira, R. C.; Buckeridge, M. O. *Carbohydr. Polym.* **2003**, *52*, 367−373.
(14) Neuman, R. D.; Berg, J. M.; Claesson, P. M. *Nordic Pulp Paper Res. J.* **1993**, *8*, 96−104.

(15) Holmberg, M.; Berg, J.; Stemme, S.; Odberg, L.; Rasmusson, J.; Claesson, P. *J. Colloid Interface Sci.* **1997**, *186*, 369−381.
(16) Holmberg, M.; Wigren, R.; Erlandsson, R.; Claesson, P. M. *Colloids Surf., A* **1997**, *130*, 175−183.
(17) Rutland, M. W.; Parker, J. L. *Langmuir* **1994**, *10*, 1110−1121.
(18) Carambassis, A.; Rutland, M. W. *Langmuir* **1999**, *15*, 5584−5590.
(19) Zauscher, S.; Klingenberg, D. J. *J. Colloid Interface Sci.* **2000**, *229*, 497−510.
(20) Zauscher, S.; Klingenberg, D. J. *Colloids Surf., A* **2001**, *178*, 213−229.
(21) Notley, S. M.; Pettersson, B.; Wagberg, L. *J. Am. Chem. Soc.* **2004**, *126*, 13930−13931.
(22) Notley, S. M.; Wagberg, L. *Biomacromolecules* **2005**, *6*, 1586−1591.
(23) Theander, K.; Pugh, R. J.; Rutland, M. W. *J. Colloid Interface Sci.* **2005**, *291*, 361−368.
(24) Berg, I. C. H.; Rutland, M. W.; Arnebrant, T. *Biofouling* **2003**, *19*, 365−369.
(25) Feiler, A.; Plunkett, M. A.; Rutland, M. W. *Langmuir* **2003**, *19*, 4173−4179.
(26) Raviv, U.; Giasson, S.; Kampf, N.; Gohy, J. F.; Jerome, R.; Klein, J. *Nature* **2003**, *425*, 163−165.
(27) Ducker, W. A.; Senden, T. J.; Pashley, R. M. *Nature* **1991**, *353*, 239−241.
(28) Ducker, W. A.; Senden, T. J.; Pashley, R. M. *Langmuir* **1992**, *8*, 1831−1836.
(29) Cleveland, J. P.; Manne, S.; Bocek, D.; Hansma, P. K. *Rev. Sci. Instrum.* **1993**, *64*, 403−405.
(30) Bogdanovic, G.; Meurk, A.; Rutland, M. W. *Colloids Surf., B* **2000**, *19*, 397−405.
(31) Feiler, A.; Attard, P.; Larson, I. *Rev. Sci. Instrum.* **2000**, *71*, 2746−2750.
(32) Ralston, J.; Larson, I.; Rutland, M. W.; Feiler, A. A.; Kleijn, M. *Pure Appl. Chem.* **2005**, *77*, 2149−2170.
(33) Verwey, E. J. W.; Overbeek, J. T. G. *Theory of the stability of lyophobic colloids: the interaction of sol particles having an electric double layer*; Elsevier: New York, 1948.
(34) Derjaguin, B. V.; Landau, L. *Acta Physiochim.* **1941**, *14*, 633−662.
(35) Bergstrom, L.; Stemme, S.; Dahlfors, T.; Arwin, H.; Odberg, L. *Cellulose* **1999**, *6*, 1−13.
(36) Chan, D. Y. C.; Pashley, R. M.; White, L. R. *J. Colloid Interface Sci.* **1980**, *77*, 283−285.
(37) Herrington, T. M.; Petzold, J. C. *Colloids Surf.* **1992**, *64*, 97−108.
(38) Rutland, M. W.; Carambassis, A.; Willing, G. A.; Neuman, R. D. *Colloids Surf., A* **1997**, *123*, 369−374.
(39) Rydholm, S. A. *Pulping Processes*; John Wiley & Sons: New York, 1965.
(40) Thompson, J. E.; Fry, S. C. *Planta* **2000**, *211*, 275−286.
(41) Stiernstedt, J.; Nordgren, N.; Wagberg, L.; Gray, D. G.; Rutland, M. W. *JCIS* **2006**, accepted.
(42) Chan, D. Y. C.; Horn, R. G. *J. Chem. Phys.* **1985**, *83*, 5311−5324.
(43) Ludwig, M.; Rief, M.; Schmidt, L.; Li, H.; Oesterhelt, F.; Gautel, M.; Gaub, H. E. *Appl. Phys. A* **1999**, *68*, 173−176.
(44) Fisher, T. E.; Marszalek, P. E.; Fernandez, J. M. *Nat. Struct. Biol.* **2000**, *7*, 719−724.
(45) Rand, R. P.; Fuller, N. L.; Lis, L. J. *Nature* **1979**, *279*, 258−260.
(46) Hoh, J. H.; Cleveland, J. P.; Prater, C. B.; Revel, J. P.; Hansma, P. K. *J. Am. Chem. Soc.* **1992**, *114*, 4917−4918.
(47) Hansma, H. G.; Hoh, J. H. *Annu. Rev. Biophys. Biomol. Struct.* **1994**, *23*, 115−139.
(48) Florin, E. L.; Moy, V. T.; Gaub, H. E. *Science* **1994**, *264*, 415−417.
(49) Leporatti, S.; Sczech, R.; Riegler, H.; Bruzzano, S.; Storsberg, J.; Loth, F.; Jaeger, W.; Laschewsky, A.; Eichhorn, S.; Donath, E. *J. Colloid Interface Sci.* **2005**, *281*, 101−111.
(50) Nigmatullin, R.; Lovitt, R.; Wright, C.; Linder, M.; Nakari-Setala, T.; Gama, A. *Colloids Surf., B* **2004**, *35*, 125−135.
(51) Morris, S.; Hanna, S.; Miles, M. J. *Nanotechnology* **2004**, *15*, 1296−1301.
(52) Parker, J. L.; Rutland, M. W. *Langmuir* **1993**, *9*, 1965−1967.
(53) Plunkett, M. A.; Rutland, M. W. *J. Adhes. Sci. Technol.* **2002**, *16*, 983−996.
(54) Derjaguin, B. V.; Toporov, Y. P. *Prog. Surf. Sci.* **1994**, *45*, 317−327.
(55) Carpick, R. W.; Ogletree, D. F.; Salmeron, M. *J. Colloid Interface Sci.* **1999**, *211*, 395−400.
(56) Feiler, A.; Larson, I.; Jenkins, P.; Attard, P. *Langmuir* **2000**, *16*, 10269−10277.
(57) Bogdanovic, G.; Tiberg, F.; Rutland, M. W. *Langmuir* **2001**, *17*, 5911−5916.
(58) Gao, J. P.; Luedtke, W. D.; Gourdon, D.; Ruths, M.; Israelachvili, J. N.; Landman, U. *J. Phys. Chem. B* **2004**, *108*, 3410−3425.
(59) Plunkett, M. A.; Feiler, A.; Rutland, M. W. *Langmuir* **2003**, *19*, 4180−4187.
(60) Rutland, M. W.; Tyrrell, J. W. G.; Attard, P. *J. Adhes. Sci. Technol.* **2004**, *18*, 1199−1215.
(61) Hertz, H. *J. Reine Angew. Math.* **1881**, *92*, 156−171.
(62) Nilsson, B.; Wagberg, L.; Gray, D. G. 12th Fundamental Research Symposium: Oxford, 2001; pp 211−224.

BM060100I